

A determinantal point process approach to scaling and local limits of random Young tableaux

Jacopo Borga¹, Cédric Boutillier², Valentin Féray^{*3}, and Pierre-Loïc
Méliot⁴

¹ *Department of Mathematics, Stanford University, United States*

² *LPSM, Sorbonne Université, France*

³ *Université de Lorraine, CNRS, IECL, F-54000 Nancy, France*

⁴ *Institut de mathématiques d'Orsay, Université Paris-Saclay, France*

Abstract. We obtain scaling and local limit results for large random multirectangular Young tableaux via the asymptotic analysis of a determinantal point process due to Gorin and Rahman (2019). In particular, we find an explicit description of the limiting surface, based on solving a complex-valued polynomial equation. As a consequence, we find a simple criterion to determine if the limiting surface is continuous in the whole domain, implying that, for multirectangular tableaux, the limiting surface is generically discontinuous.

1 Introduction

Random Young diagrams form a classical theme in probability theory, starting with the work of Logan–Shepp and Vershik–Kerov on the Plancherel measure [12, 19]. The topic is deeply connected with random permutations, random matrix theory and particle systems, and has known an increase of interest after the discovery of an underlying determinantal point process for a Poissonized version of the Plancherel measure [4]. It would be vain to do a complete review of the related literature, and we refer only to [8, 17] for books on the topic.

In comparison, random Young tableaux have a shorter history. Motivations to study random Young tableaux range from asymptotic representation theory to connections with other models of combinatorial probability, such as random permutations with short monotone subsequences [16] or most notably random sorting networks; see e.g. [1].

As in most of the literature, we are interested in the simple model where we fix a partition λ (or rather a sequence of growing partitions) and consider a uniform random tableau T of shape λ . In [14], Pittel and Romik derived a limiting surface result for uniform random Young tableaux of rectangular shapes, based on the hook length formula

^{*}valentin.feray@univ-lorraine.fr. This is an extended abstract of [3], submitted elsewhere.

and analytic arguments. An earlier result of Biane in asymptotic representation theory [2] implies, in fact, the existence of such limiting surfaces for any underlying shape. However, getting explicit formulas for these limiting surfaces is difficult since their description involves the Markov–Krein correspondence and the free compression of probability measures. More recently, entropy optimization methods have been applied to prove the existence of limiting surfaces, extending the result to skew shapes [18]. These techniques lead to some natural gradient variational problems in \mathbb{R}^2 whose solutions are explicitly parameterized by κ -harmonic functions, as shown in [10].

Recently, in [5], a determinantal point process structure was discovered for a Poissonized version of random Young tableaux. This determinantal structure was used for a specific problem motivated by the aforementioned sorting networks, namely describing the local limit of uniform tableaux of staircase shape around their outer diagonal [5, 6].

The goal of the current paper is to exploit this determinantal point process structure in order to get limiting results for a large family of shapes. Namely, we consider shapes obtained as dilatations of any given Young diagram λ^0 , i.e. multirectangular diagrams. Here is an informal description of our results.

- We obtain a new description of the limiting surface corresponding to the shape λ^0 , based on solving a complex-valued polynomial equation (Theorem 4). This new description is more explicit compared to the one obtained through the existence approaches.
- This first result leads us to a surprising discontinuity phenomenon for the limiting surface corresponding to λ^0 . More precisely, we establish a simple criterion – some equations involving the so-called *interlacing coordinates* of λ^0 – to determine whether the limiting surface is continuous (Theorem 6). This shows that such limiting surfaces are typically discontinuous for multirectangular tableaux.
- We also obtain a local limit result in the bulk of random Young tableaux. Due to space constraints, we do not present this result in this extended abstract and refer the interested reader to the long version of the article [3].

Remark 1. *In parallel to this work, explicit formulas for the limiting surfaces of random Young tableaux have also been obtained by Prause [15] through a different method (solving a variational problem obtained by the tangent plane method of Kenyon and Prause [10]).*

2 Results

2.1 Young tableaux and height function

Let us start by fixing terminology and notation. A *partition* of n is a non-increasing list $\lambda = (\lambda_1, \lambda_2, \dots, \lambda_l)$ of positive integers with $N = \sum_{i=1}^l \lambda_i$. We write $|\lambda| = N$ for the *size*

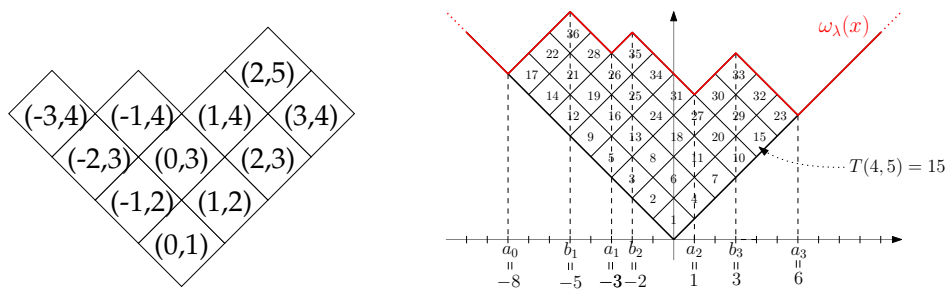


Figure 1: **Left:** The Young diagram of the partition $(4, 4, 2, 1)$ drawn in Russian convention, with the coordinates of each box inside it. **Right:** A Young tableau $T : \lambda \rightarrow [N]$ of shape λ corresponding to the partition $(6, 6, 6, 4, 4, 4, 3, 3)$ drawn according to the Russian convention; all the boxes are squares with area 2. We indicate the interlacing coordinates $a_0 < b_1 < a_1 < b_2 < \dots < b_m < a_m$ below the x -axis.

of the partition and $\ell(\lambda) = l$ for the *length* of the partition and use the convention $\lambda_i = 0$ when $i > \ell(\lambda)$. We represent partitions graphically with the *Russian convention*, i.e. for each $i \leq \ell(\lambda)$ and $j \leq \lambda_i$ we have a square box whose sides are parallel to the lines $x = y$ and $x = -y$ and whose center has coordinates $(j - i, i + j - 1)$; see the left-hand side of [Figure 1](#). This graphical representation is called *Young diagram* of shape λ .

When looking at a Young diagram λ , its upper boundary is the graph of a 1-Lipschitz function, denoted by $\omega_\lambda : \mathbb{R} \rightarrow \mathbb{R}$, and the diagram λ can be encoded using the local minima and maxima of the function ω_λ . Following Kerov [[11](#)], we denote them by

$$a_0 < b_1 < a_1 < b_2 < \dots < b_m < a_m, \quad a_i, b_i \in \mathbb{Z}, \quad (2.1)$$

and we call them *interlacing coordinates*. See the right-hand side of [Figure 1](#) for an example. Note that $a_0 = -\ell(\lambda)$ and $a_m = \lambda_1$. Furthermore, interlacing coordinates satisfy $\sum_{i=0}^m a_i = \sum_{i=1}^m b_i$, see, e.g., [[9](#), Proposition 2.4].

A *Young tableau* of shape λ is a filling of the boxes of λ with the numbers $1, 2, \dots, N$ such that the numbers along every row or column are increasing. We see Young tableaux as functions $T : \lambda \rightarrow [N] = \{1, 2, \dots, N\}$, where the Young diagram λ is identified with the set $\{(j - i, i + j - 1), i \leq \ell(\lambda), j \leq \lambda_i\}$; see again the right-hand side of [Figure 1](#) for an example. The function $T : \lambda \rightarrow [N]$ can be thought of as the graph of a (non-continuous) surface above the set λ .

We also represent a tableau T of size N by its *height function* H_T (normalized in the second argument). It is a map from $([a_0, a_m] \cap \mathbb{Z}) \times [0, 1]$ to $\mathbb{Z}_{\geq 0}$ defined by

$$H_T(x, t) = \# \{y : T(x, y) \leq Nt\}, \quad (2.2)$$

i.e. $H_T(x, t)$ is the number of entries smaller than Nt in the vertical line $\{x\} \times \mathbb{Z}_{\geq 0}$. Clearly, the tableau T is entirely determined by the height function H_T . Moreover, we

have that

$$T(x, y) < Nt \quad \text{if and only if} \quad H(x, t) > \frac{1}{2}(y - |x|). \quad (2.3)$$

2.2 Previous results: existence of a limiting height function

We now look at growing Young diagrams, and the associated random tableaux. We fix a Young diagram λ^0 , and take our growing sequence of diagrams as dilatations of λ^0 . Namely, for $n > 0$, we define $N = N(n, \lambda^0) = n^2 |\lambda^0|$ and consider the $(n \times n)$ -dilated diagram λ_N obtained by replacing each box of λ^0 by a square of $n \times n$ boxes. Note that λ_N has size N . We set $\eta = 1/\sqrt{|\lambda^0|}$, so that scaling λ^0 in both directions by a factor η gives a diagram of area 2. Finally, we let T_N be a uniform random Young tableau of shape λ_N .

The following convergence result for the height function of T_N is proved in [18, Theorem 7.15]. It also follows indirectly from earlier concentration results on random Young diagrams by Biane [2]; see [13, Proposition 10.1].

Theorem 2 ([18, Theorem 7.15] and [13, Proposition 10.1]). *Let λ^0 be a fixed Young diagram and a_0, \dots, a_m be its interlacing coordinates as defined in (2.1). We let T_N be a uniform random Young tableau of shape λ_N . Then there exists a deterministic function $H^\infty : [\eta a_0, \eta a_m] \times [0, 1] \rightarrow \mathbb{R}$ such that the following convergence in probability holds:*

$$\frac{1}{\sqrt{N}} H_{T_N} \left(\lfloor x\sqrt{N} \rfloor, t \right) \xrightarrow{N \rightarrow +\infty} H^\infty(x, t), \quad (2.4)$$

uniformly for all (x, t) in $[\eta a_0, \eta a_m] \times [0, 1]$.

In [18], the limiting function H^∞ is implicitly found to be the unique maximizer of a certain entropy functional subject to some boundary conditions depending on the diagram λ^0 . Using the approach of [2, 13], for each $t \in [0, 1]$, the section $H^\infty(\cdot, t)$ is described using the free cumulants of an associated probability measure. Both descriptions are difficult to manipulate. Our first result gives an alternative and more explicit description of H^∞ through the solution of a polynomial equation, called the *critical equation*.

2.3 First result: a compact description of the limiting height function

Let $a_0 < b_1 < a_1 < b_2 < \dots < a_m$ be the interlacing coordinates of λ^0 , introduced in (2.1). For (x, t) in $[\eta a_0, \eta a_m] \times [0, 1]$, we consider the following polynomial equation, referred to throughout the paper as the *critical equation*:

$$U \prod_{i=1}^m (x - \eta b_i + U) = (1 - t) \prod_{i=0}^m (x - \eta a_i + U). \quad (2.5)$$

This is a polynomial equation in the complex variable U of degree $m + 1$. Using the fact that the a_i 's and b_i 's are alternating, one can easily prove that (2.5) has at least $m - 1$ real solutions; see [3, Lemma 24] for details. Hence it has either 0 or 2 non-real solutions.

Definition 3. We let L be the set of pairs (x, t) in $[\eta a_0, \eta a_m] \times [0, 1]$ such that (2.5) has two non-real solutions and we call it liquid region. The complement of the liquid region in $[\eta a_0, \eta a_m] \times [0, 1]$ will be referred to as the frozen region.

For $(x, t) \in L$, we denote by $U_c = U_c(x, t)$ the unique solution with a positive imaginary part of the critical equation (2.5). We use the notation $\Re z$ and $\Im z$ for the real and imaginary parts of the complex number z . It turns out that the limiting height function H^∞ is expressed in terms of U_c using the following simple formula.

Theorem 4. With the above notation, for $(x, t) \in [\eta a_0, \eta a_m] \times [0, 1]$, we have

$$H^\infty(x, t) = \frac{1}{\pi} \int_0^t \frac{\Im U_c(x, s)}{1 - s} \mathbf{1}[(x, s) \in L] ds.$$

Informally, the liquid region is the limit of the region where the height function H_{T_N} is strictly increasing in the t -direction, and the t -derivative of H_{T_N} in this region is roughly given by $\sqrt{N} \Im U_c(x, s) / (\pi(1 - s))$.

2.4 Limiting surfaces and discontinuities

It is natural to try to translate the limiting result for the height function to a limit result for the tableau itself, seen as a discrete surface. Namely, we set

$$D_{\lambda^0} := \left\{ (x, y) \in \mathbb{R}^2 : |x| < y < \eta \omega_{\lambda^0}(x/\eta) \right\}, \quad (2.6)$$

which is the open domain of \mathbb{R}^2 corresponding to the diagram λ^0 (in Russian convention), normalized to have area 2. For (x, y) in D_{λ^0} , letting T_N be a uniform tableau of shape λ_N , we consider

$$\tilde{T}_N(x, y) := \frac{1}{N} T_N \left(\lfloor x\sqrt{N} \rfloor, \lfloor y\sqrt{N} \rfloor + \delta \right), \quad (2.7)$$

where $\delta \in \{0, 1\}$ is chosen so that the arguments of T_N have distinct parities. We want to find a scaling limit for the function $\tilde{T}_N(x, y)$. To this end, we set for all $(x, y) \in D_{\lambda^0}$,

$$\begin{aligned} T_+^\infty &= T_+^\infty(x, y) := \sup \left\{ t \in [0, 1] : H^\infty(x, t) \leq \frac{1}{2}(y - |x|) \right\}, \\ T_-^\infty &= T_-^\infty(x, y) := \inf \left\{ t \in [0, 1] : H^\infty(x, t) \geq \frac{1}{2}(y - |x|) \right\}. \end{aligned} \quad (2.8)$$

Comparing Equations (2.3) and (2.8), the following statement is an easy consequence of Theorem 2, see [3] for details.

Proposition 5. *For all $\varepsilon > 0$, the following limit holds uniformly for all $(x, y) \in D_{\lambda^0}$:*

$$\lim_{N \rightarrow +\infty} \mathbb{P}(\tilde{T}_N(x, y) < T_-^\infty - \varepsilon) = \lim_{N \rightarrow +\infty} \mathbb{P}(\tilde{T}_N(x, y) > T_+^\infty + \varepsilon) = 0.$$

We let $D_{\lambda^0}^{\text{reg}}$ be the set of coordinates $(x, y) \in D_{\lambda^0}$ such that $T_-^\infty(x, y) = T_+^\infty(x, y)$. For such points, we simply write $T^\infty(x, y)$ for this common value. Then Proposition 5 implies the following convergence in probability for $(x, y) \in D_{\lambda^0}^{\text{reg}}$:

$$\lim_{N \rightarrow +\infty} \tilde{T}_N(x, y) = T^\infty(x, y), \quad (2.9)$$

On the other hand, for (x, y) in $D_{\lambda^0} \setminus D_{\lambda^0}^{\text{reg}}$, we do not know whether $\tilde{T}_N(x, y)$ converges at all, and the limiting surface T^∞ is discontinuous at such points.

A natural question is whether such discontinuity points (x, y) exist at all in D_{λ^0} . Our second main result shows that such points indeed exist unless λ^0 is a rectangle, or unless its interlacing coordinates satisfy some specific equations.

Theorem 6. *For a Young diagram λ^0 , the following assertions are equivalent:*

1. *The limiting surface T^∞ is continuous in the whole domain D_{λ^0} ;*
2. *The interlacing coordinates defined in (2.1) satisfy the system of equations:*

$$\sum_{\substack{i=0 \\ i \neq i_0}}^m \frac{1}{a_{i_0} - a_i} = \sum_{i=1}^m \frac{1}{a_{i_0} - b_i}, \quad \text{for all } i_0 = 1, \dots, m-1. \quad (2.10)$$

Note that when $m = 1$, i.e. when λ^0 has a rectangular shape, there are no equations in the second item. Indeed, the limiting surface T^∞ is always continuous in this case. For $m > 1$ however, the limiting surface is generically discontinuous.

3 Examples

In this section, we illustrate our results in the cases $m = 1$ (rectangular shapes) and $m = 2$ (L -shapes). Before starting, let us note that our model and all results are invariant when multiplying all interlacing coordinates of λ^0 by the same positive integers. We will therefore allow ourselves to work with diagrams λ^0 with rational (non-necessarily integer) interlacing coordinates.

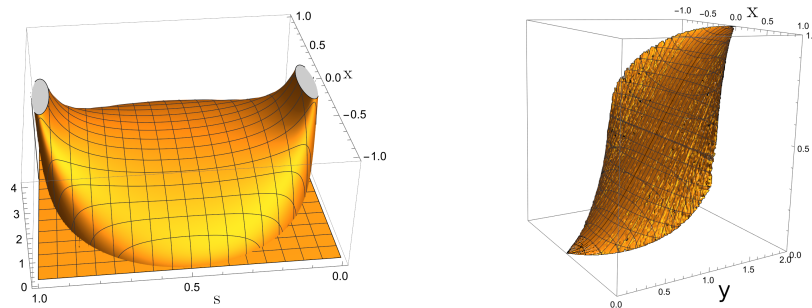


Figure 2: **Left:** The graphs of the function $\alpha(x, s) = \frac{\sqrt{4s-4s^2-x^2}}{2s-2s^2}$ from Remark 8. **Right:** The corresponding limiting surface $T_1^\infty(x, y)$ for squared diagrams. Note that we are using two different orientations of axes in order to improve the visualization.

3.1 An explicit formula for the rectangular case

In this section, we consider a rectangular diagram λ_0 . Without loss of generality, we assume $a_0 = -1$ and write $r = a_1$. Necessarily, $b_1 = r - 1$. Solving explicitly the critical equation (2.5), which is in this case a degree 2 polynomial equation, we get:

Proposition 7. *The limiting height function corresponding to a $1 \times r$ rectangular shape λ^0 is given by*

$$H_r^\infty(x, t) = \frac{1}{\pi} \int_0^t \frac{\sqrt{s(4r - (1+r)^2s) + 2(r-1)\sqrt{rs}x - rx^2}}{2\sqrt{r}(1-s)s} ds \tag{3.1}$$

with the convention that $\sqrt{x} = 0$ if $x \leq 0$. Furthermore, the limiting surface T_r^∞ is continuous on D_{λ^0} and is therefore implicitly determined by the equation

$$H_r^\infty(x, T_r^\infty(x, y)) = \frac{1}{2}(y - |x|). \tag{3.2}$$

Remark 8. *In the case $r = 1$ (square Young tableaux), we get*

$$H_1^\infty(x, t) = \frac{1}{\pi} \int_0^t \frac{\sqrt{4s - 4s^2 - x^2}}{2s - 2s^2} ds.$$

The graph of the function $\alpha(x, s) = \frac{\sqrt{4s-4s^2-x^2}}{2s-2s^2}$ is plotted on the left-hand side of Figure 2, while the corresponding limiting surface T_1^∞ is on the right. The above integral can be explicitly computed, recovering the formula found by Pittel and Romik from [14]. Pittel and Romik also give formulas for the general rectangular case, which should coincide with (3.1), though we could not verify directly the equivalence of both formulae.

One can also obtain explicit formulas for L-shaped diagrams; since the latter expressions are involved, we decided not to display them, and to discuss examples instead.

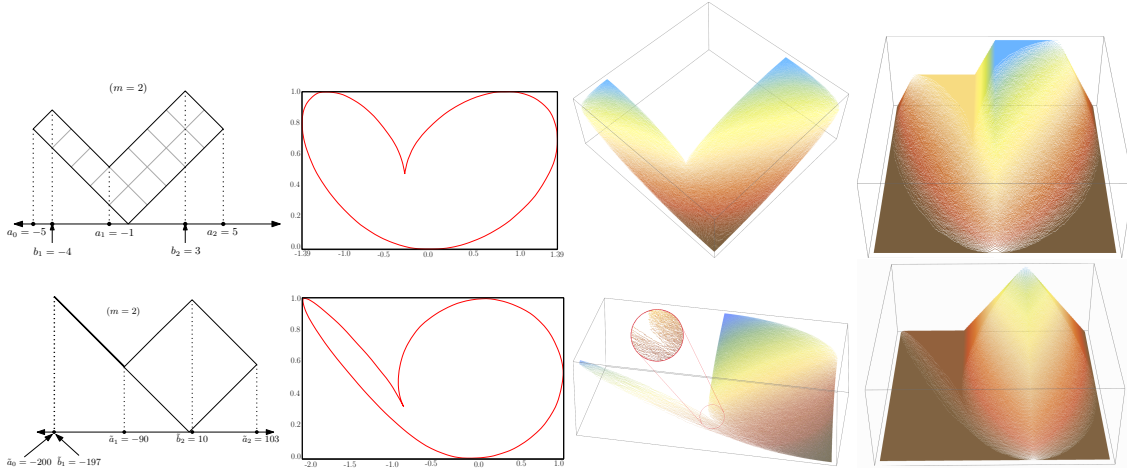


Figure 3: Figures for the heart example (top row) and for the pipe example (bottom row). **In each row, from left to right:** The Young diagram λ^0 or $\tilde{\lambda}^0$ with its interlacing coordinates, the boundary curve of the corresponding liquid region, a uniform random tableau T_N of shape λ_N (with respectively $N = 130000$ and $N = 59400$ boxes) and the corresponding height function H_{T_N} (in 3D plots, the brown colour is used for small values of the surface and blue for large ones).

3.2 Two concrete examples of L -shape diagrams

We now consider two specific diagrams λ^0 and $\tilde{\lambda}^0$ which are both L -shaped (i.e. $m = 2$). Due to the shape of the corresponding liquid regions (see the pictures in Figure 3), the first one is called the *heart example* and the second one the *pipe example*.

In the heart example, the Young diagram λ^0 has interlacing coordinates

$$a_0 = -5 < b_1 = -4 < a_1 = -1 < b_2 = 3 < a_2 = 5. \quad (3.3)$$

In this case we have $|\lambda^0| = 13$, so that $\eta = 1/\sqrt{|\lambda^0|} = 1/\sqrt{13}$ and $[\eta a_0, \eta a_m] = [-5/\sqrt{13}, 5/\sqrt{13}] \approx [-1.39, 1.39]$.

In the pipe example, the Young diagram $\tilde{\lambda}^0$ has interlacing coordinates

$$\tilde{a}_0 = -200 < \tilde{b}_1 = -197 < \tilde{a}_1 = -90 < \tilde{b}_2 = 10 < \tilde{a}_2 = 103. \quad (3.4)$$

In this case, we have $|\tilde{\lambda}^0| = 9900$, so that $\tilde{\eta} = \frac{1}{30\sqrt{11}}$ and $[\tilde{\eta}\tilde{a}_0, \tilde{\eta}\tilde{a}_m] = [-\frac{200}{30\sqrt{11}}, \frac{103}{30\sqrt{11}}] \approx [-2.01, 1.04]$.

For both examples, we have computed the boundary of the liquid region defined in Definition 3. Independently, we have also generated a uniform random tableau of shape λ_N for large N (using the Greene–Nijenhuis–Wilf hook walk algorithm [7]), and we present 3D plots both of the tableau T as a function from λ to $[0, 1]$ and of its height

function H_T (which is a function from $[na_0, na_m] \times [0, 1]$ to $\mathbb{Z}_{\geq 0}$). In both cases, the domain where the height function H_T is increasing in t fits very well with the liquid region, as predicted by [Theorem 4](#).

An essential difference between the two examples is that the interlacing coordinates satisfy [Condition \(2.10\)](#) in the heart example, while this is not the case in the pipe example. From [Theorem 6](#), the limiting surface is continuous in the heart example and not in the pipe example. This is indeed visible on the pictures, as we now explain.

In the heart example, the intersection of the liquid region with any vertical line is connected; in other terms, for every $x \in [\eta a_0, \eta a_m]$, the function $t \mapsto H^\infty(x, t)$ is first constant equal to 0, then strictly increasing, and then constant equal to its maximal value. Therefore, with the notation of [\(2.8\)](#), we have $T_-^\infty(x, y) = T_+^\infty(x, y)$ for all (x, y) in D_{λ^0} and the limiting surface T^∞ is defined and continuous on the whole set D_{λ^0} . Looking at the random tableau drawn as a discrete surface, it is indeed plausible that it converges to a continuous surface.

In the pipe example, however, we can find some x_0 just on the right of $\eta \tilde{a}_1 = -\frac{3}{\sqrt{11}} \approx -0.9$ so that the liquid region intersects the line $x_0 \times [0, 1]$ in two disjoint intervals. The function $t \mapsto H^\infty(x_0, t)$ is then constant, equal to some value y_0 between these two intervals. It follows that $T_-^\infty(x_0, y_0) < T_+^\infty(x_0, y_0)$ and the limiting surface T^∞ is discontinuous at (x_0, y_0) . This discontinuity can be observed on the 3D plot of the tableau T_N (see the zoom inside the red circle on the left-hand side, where we observe a jump in the values of T_N).

4 Proof strategy

We now discuss the proof strategy of [Theorems 4](#) and [6](#). Details can be found in [\[3\]](#).

4.1 Poissonized tableaux and determinantal point process

Following [\[5\]](#), we define a *Poissonized Young tableau* of shape λ as a function $\lambda \rightarrow [0, 1]$ satisfying the same monotonicity constraints as standard tableaux. We encode such a tableau T by a set M_T of particles in $\mathbb{Z} \times [0, 1]$ defined as

$$M_T = \{(x, T(x, y)), (x, y) \in \lambda\}.$$

A remarkable result of [\[5\]](#) states that, for any shape λ , if T is a uniform random Poissonized tableau of shape λ , then M_T is a determinantal point process with kernel

$$K_\lambda((x_1, t_1), (x_2, t_2)) = -\frac{1}{(2i\pi)^2} \oint_{\gamma_z} \oint_{\gamma_w} \frac{F_\lambda(z)}{F_\lambda(w)} \frac{\Gamma(w-x_1+1)}{\Gamma(z-x_2+1)} \frac{(1-t_2)^{z-x_2} (1-t_1)^{-w+x_1-1}}{z-w} dw dz, \quad (4.1)$$

where

- $F_\lambda(u) := \Gamma(u+1) \prod_{i=1}^{\infty} \frac{u+i}{u-\lambda_i+i} = \frac{\prod_{i=0}^m \Gamma(u-a_i+1)}{\prod_{i=1}^m \Gamma(u-b_i+1)}$;
- γ_w and γ_z are counterclockwise contours containing all the integers in $[a_0, x_1]$ and in $[x_2, a_m]$ respectively;
- γ_w and is inside (resp. outside) γ_z if $t_1 \geq t_2$ (resp. $t_1 < t_2$);
- the ratio $\frac{1}{z-w}$ remains uniformly bounded on the contours γ_w and γ_z .

4.2 Asymptotic behaviour of the kernel

To prove [Theorem 4](#), we look for the asymptotic behaviour of the kernel in the regime

$$x_i = x_0\sqrt{N} + \xi_i, \quad t_i = t_0 + \frac{\tau_i}{\sqrt{N}} \quad (i = 1, 2),$$

where (x_0, t_0) is fixed in $[\eta a_0, \eta a_m] \times [0, 1]$. In particular, the density of particles in M_T around $(x_0\sqrt{N}, t_0)$, normalized by $1/\sqrt{N}$, is given by $K_\lambda((x_0\sqrt{N}, t_0), (x_0\sqrt{N}, t_0))$, corresponding hence to $\xi_1 = \xi_2 = \tau_1 = \tau_2 = 0$. In this regime, a careful asymptotic analysis shows that the integrand in [Equation \(4.1\)](#) behaves as

$$\text{Int}_N(W, Z) \simeq (\sqrt{N})^{\xi_2 - \xi_1} e^{\sqrt{N}(S(W) - S(Z))} h(W, Z), \quad (4.2)$$

for some function S and h . The critical equation [\(2.5\)](#) corresponds to the equation $S'(U) = 0$, i.e. its solutions are critical points of S . The idea is then to move the integration contours so that $S(W) < S(Z)$ on the new contours, making the integrand and thus the integral tend to 0. Moving the integration contour may yield a residue term, which gives the non-trivial asymptotic of $K_\lambda((x_0\sqrt{N}, t_0), (x_0\sqrt{N}, t_0))$.

Let us explain briefly how this works when (x_0, t_0) is in the liquid region. By definition, in this case, S has two non-real critical points, which are necessarily conjugate, that we denote by U_c and \bar{U}_c . Comparing $\Re S(U)$ (for generic U) to $\Re S(U_c)$ divides the complex plane into regions as shown on [Figure 4](#) (the shape of those regions is carefully justified in the long version of the paper [\[3\]](#)). We then move the integration contours so that $S(W) < S(U_c) < S(Z)$ almost everywhere on the new contours. Note that the new contour γ_W^{new} is not inside γ_Z^{new} , while γ_w is inside γ_z since $t_1 = t_2$ in the case of interest. Thus moving the contours yields a residue term associated with the pole $Z = W$ in [Equation \(4.1\)](#), which can be computed explicitly. We find

$$\lim_{N \rightarrow +\infty} K_\lambda((x_0\sqrt{N}, t_0), (x_0\sqrt{N}, t_0)) = \frac{\Im U_c(x_0, t_0)}{\pi(1-t_0)},$$

which implies after some work [Theorem 4](#).

We note that the general proof strategy is standard in integrable probability but needs many careful estimations and arguments to justify the existence of the appropriate contours, and the asymptotic behaviour of the various terms (see [\[3\]](#)).

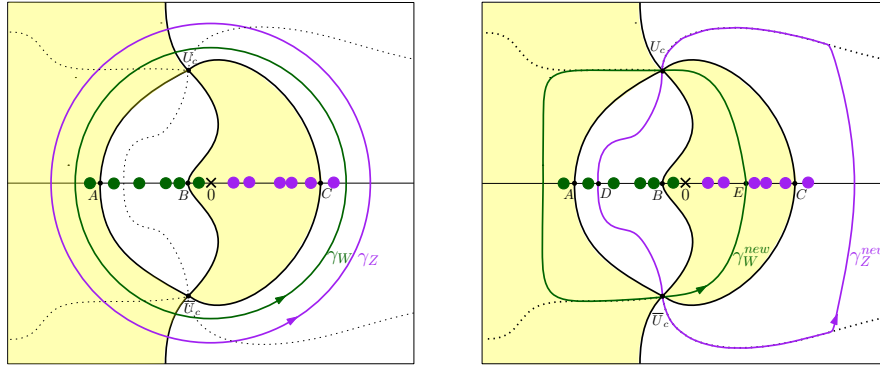


Figure 4: Left: The yellow regions correspond to $\{\Re S(U) < \Re S(U_c)\}$, while the white regions correspond to $\{\Re S(U) > \Re S(U_c)\}$. We plotted the original integration contours γ_W (in green) and γ_Z (in purple) appearing in Equation (4.1). The green and purple dots are respectively the W -poles and Z -poles of the integrand. **Right:** The new integration contours so that $S(W) < S(Z)$ almost everywhere on the contours.

4.3 Characterization of continuous limit shapes

We now discuss the proof of Theorem 6. Looking at the shape of the liquid regions in Figure 3 and at the discussions on the heart and pipe examples, we see that the limit shape is continuous if and only if the tangent vectors to the boundary of the liquid region at its cusp points are all vertical. The boundary of the liquid region is precisely the set of points (x, t) where the discriminant of the polynomial equation (2.5) vanishes, see [3, Proposition 27]. Using this description, we can obtain an explicit parametrization of this boundary curve, and compute the tangent vectors at its cusp points. Each cusp point gives one of the condition given in Equation (2.10), concluding the proof of the theorem.

References

- [1] O. Angel, A. E. Holroyd, D. Romik, and B. Virág. “Random sorting networks”. *Adv. Math.* **215.2** (2007), pp. 839–868. [DOI](#).
- [2] P. Biane. “Approximate factorization and concentration for characters of symmetric groups”. *Internat. Math. Res. Notices* **4** (2001), pp. 179–192.
- [3] J. Borga, C. Boutillier, V. Féray, and P.-L. Méliot. “A determinantal point process approach to scaling and local limits of random Young tableaux”. 2023. [arXiv:2307.11885](#).
- [4] A. Borodin, A. Okounkov, and G. Olshanski. “Asymptotics of Plancherel measures for symmetric groups”. *J. Amer. Math. Soc* **13** (2000), pp. 481–515.

- [5] V. Gorin and M. Rahman. “Random sorting networks: local statistics via random matrix laws”. *Probab. Theory Relat. Fields* **175**.1-2 (2019), pp. 45–96.
- [6] V. Gorin and J. Xu. “Random sorting networks: edge limit”. 2022. [arXiv:2207.09000](https://arxiv.org/abs/2207.09000).
- [7] C. Greene, A. Nijenhuis, and H. Wilf. “A probabilistic proof of a formula for the number of Young tableaux of a given shape”. *Young Tableaux in Combinatorics, Invariant Theory, and Algebra*. Elsevier, 1982, pp. 17–22.
- [8] A. Hora. *The limit shape problem for ensembles of Young diagrams*. Vol. 17. SpringerBriefs Math. Phys. Tokyo: Springer, 2016. [DOI](#).
- [9] V. Ivanov and G. Olshanski. “Kerov’s central limit theorem for the Plancherel measure on Young diagrams”. *Symmetric functions 2001: surveys of developments and perspectives*. Vol. 74. NATO Sci. Ser. II Math. Phys. Chem. Dordrecht: Kluwer Acad. Publ., 2002, pp. 93–151.
- [10] R. Kenyon and I. Prause. “Gradient variational problems in \mathbb{R}^2 ”. *Duke Math. J.* **171**.14 (2022), pp. 3003–3022. [DOI](#).
- [11] S. V. Kerov. “Anisotropic Young diagrams and Jack symmetric functions”. *Funct. Anal. Appl.* **34**.1 (2000), pp. 41–51. [DOI](#).
- [12] B. F. Logan and L. A. Shepp. “A variational problem for random Young tableaux”. *Advances in Math.* **26**.2 (1977), pp. 206–222.
- [13] Ł. Maślanka and P. Śniady. “Second class particles and limit shapes of evacuation and sliding paths for random tableaux.” *Doc. Math.* **27** (2022), pp. 2183–2273. [DOI](#).
- [14] B. Pittel and D. Romik. “Limit shapes for random square Young tableaux”. *Adv. Appl. Math.* **38**.2 (2007), pp. 164–209. [DOI](#).
- [15] I. Prause. “Random Young tableaux and the tangent plane method”. in preparation. 2023.
- [16] D. Romik. “Permutations with short monotone subsequences”. *Adv. Appl. Math.* **37** (2006), pp. 501–510.
- [17] D. Romik. *The surprising mathematics of longest increasing subsequences*. Vol. 4. Institute of Mathematical Statistics Textbooks. Cambridge University Press, 2015.
- [18] W. Sun. “Dimer model, bead model and standard Young tableaux: finite cases and limit shapes”. 2018. [arXiv:1804.03414](https://arxiv.org/abs/1804.03414).
- [19] A. M. Vershik and S. V. Kerov. “Asymptotic behavior of the Plancherel measure of the symmetric group and the limit form of Young tableaux”. *Dokl. Akad. Nauk SSSR* **233**.6 (1977), pp. 1024–1027.